Disordered ultracold quantum gases

Master Thesis
submitted to the Faculty of the
Escola Tècnica d'Enginyeria de Telecomunicació de Barcelona
Universitat Politècnica de Catalunya
by

Pau Fargas Reixats

In partial fulfillment
of the requirements for the master in
Engineering Physics

Advisor: Dr. Pietro Massignan
Coadvisor: Dr. Grigori Astrakharchik
Barcelona, Date 1st of July, 2024

Contents

1 Introduction **5**
1.1 Localization phenomena in condensed matter physics . . . 5
1.2 Objectives . . . 6
1.3 Procedure and setbacks . . . 6
1.4 Units . . . 6
1.5 Gantt Diagram . . . 7

2 State of the art **8**
2.1 Anderson localization . . . 8
2.2 Ultracold atoms for quantum simulation . . . 9
2.3 The pseudopotential approximation. Conditions in the wave function . . . 9
2.4 The Fermi gas: Non-interacting fermions . . . 11

3 Methodology **13**
3.1 Framework used in this work . . . 13
3.2 Criterium for localization . . . 13
3.3 Scaling theory: 2D as a critical dimension . . . 14
3.4 Formulation of the problem . . . 15
3.4.1 Wavefunction of a resonance . . . 18
3.5 Finding resonances . . . 18

4 Results **20**
4.1 Optimization of the code . . . 20
4.2 Density of localized states . . . 20
4.3 The wavefunction . . . 22
4.4 Non-interacting fermions . . . 24

5 Budget **26**

6 Environment Impact **27**

7 Conclusions and future development **28**

Appendices **29**

A Two dimensional scattering: binary collisions **29**
A.1 Variable separation, diffusion amplitude . . . 29
A.2 The diffusion amplitude in 3D . . . 31
A.3 The diffusion amplitude in 2D . . . 33

B Green's function **36**
B.1 Definition . . . 36
B.2 Green's function in quantum mechanics: The single particle propagator . . . 37

References **41**

Revision history and approval record

Revision	Date	Purpose
0	13/05/2024	Document creation
1	27/06/2024	Document revision
2	01/07/2024	Document revision

DOCUMENT DISTRIBUTION LIST

Name	e-mail
Pau Fargas Reixats	
Dr. Pietro Massignan	
Dr. Grigori Astrakharchik	

Written by:		Reviewed and approved by:	
Date	01/07/2024	Date	01/07/2024
Name	Pau Fargas Reixats	Name	Pietro Massignan
Position	Project Author	Position	Project Supervisor

Abstract

Localisation in condensed matter physics is one of the pillars of understanding the transport properties of materials, like conductivity in solids.In this thesis, we explore Anderson localisation of a Fermi gas in a 2D disordered media of point-like scatterers, using the propagator's formulation of quantum mechanics. We find the density of localized states and some examples of localized wavefunctions.

1 Introduction

The *wave-particle duality* is one of the most famous behaviours that arise when considering particles in the quantum regime. The Schrödinger equation treats quantum objects as a complex wave, *the wavefunction of the particle*, the physical interpretation of which is that the square of this wavefunction represents the probability distribution function of the position of the quantum object.

This new way of understanding particles makes wave phenomena possible, like interference when two particles interact with each other or diffusion in a medium. In this work, we study a wave phenomenon called *localization*, or the absence of difusion of a wave.

In the classical sense, particles are localized if their energy is less than the maximum potential $E < V_{max}$: they have a defined position, but for a wave, this statement might not be true: In general, waves span over a large region, for example, if we emit an electromagnetic wave from a source into an empty universe this wave will be propagated throughout all space. Using the interference of different waves, one can also find localised waves, such as the *wave packet*.

The aim of this work is to characterize the localization of non interacting fermions in a disordered media of scatterers in the low energy approximation, by computing the density of bound states given a scattering length a_{eff} and a Fermi energy E_F. The system is modelled as a set of point-like scatterers in a 2D simple cubic circular lattice.

1.1 Localization phenomena in condensed matter physics

Arguably, the most known model for lattice systems that presents localization is the Hubbard model. In it, the dynamic of the particles are described by the interplay between the kinetic (or tunneling) and interparticle interaction energies. The Hubbard model is a simplified model that can describe the electronic structure of solids, where the electrons are confined to a lattice of atoms. The electrons can hop between the lattice sites and interact with each other when they are in the same site. If the interaction energy is much larger than the kinetic energy, the electrons will be localized in the lattice sites and the system will be an insulator. This phase of matter is called the Mott insulator phase and the localized character is due to repulsion between particles, meaning there is a need for many interacting particles to lead to localization.

However, in disordered systems, the backscattering effects of a single particle with the disorder, can lead to a constructive interference of the wavefunction in some region of space, reducing the conductivity of the material in case of solid state materials. This is called weak localization and it is considered the precursor of the Anderson localization or strong localization phenomena.

Anderson localization, or strong localization, is a wave phenomena in which the wavefunction of a particle is a square integrable function and decays exponentially far away. This means that the particle is confined in a region of space, in which classically it should not be localized. More details are given in the next section.

1.2 Objectives

In this work we aim to study the localization of a non-interacting Fermi gas in a 2D lattice of point-like scatterers. The main objectives are:

1. Understand Anderson localization and 2D scattering theory.
2. Implement a Green's function based approach to the problem, based on [1] and [2], and try to reproduce their results.
3. Build the resonant wavefunctions and see the localization of the states.
4. Extend the argument to a system of non-interacting fermions, by computing its spectrum through the diagonalization of the Hamiltonian.

1.3 Procedure and setbacks

Even though the formalism could be somewhat intimidating, and the theory of scattering in 2D is not trivial, if we take the results obtained in 2D in [2] the problem is simplified to an easy mathematical problem. However, the fact that we were not working with tools like Mathematica or Matlab, but with Python, made the implementation to be more challenging. Those kinds of scientific numerical software have a lot of built-in functions that can be directly used, such as code parallelisation or matrix operations. In the case of python, we had to investigate which libraries, techniques and data representation was the best for the problem.

Finally, the combination of vectorization of the operations with numpy, and parallelisation of the code using the multiprocessing library and numba, made the code fast enough to be useful.

The main setback of this work was the lack of experience in the formalism used, and the poor implementation of the own code. The first iteration of the code was too slow to be useful, due to the lack of knowledgement in optimization techniques. There has been a lot of time spent in understanding the formalism and the optimization of the code, with multiple tries in the code.

1.4 Units

The disordered system that we will be working with will be a circular simple cubic (4 nearest neighbours) lattice of dispersors with a distance between nearest neighbours d. The characteristic energy of the system is $E_0 = \frac{\hbar^2}{md^2}$, meaning that the characteristic time of the system is $\tau_0 = \hbar/E_0$. For the simulations, the units used are $\hbar = 1$, $m = 1$ and $d = 1$. The energy of the system is then measured in units of E_0. That means that the wavevector k can be expressed as function of the energy as $k = \sqrt{2E}$.

1.5 Gantt Diagram

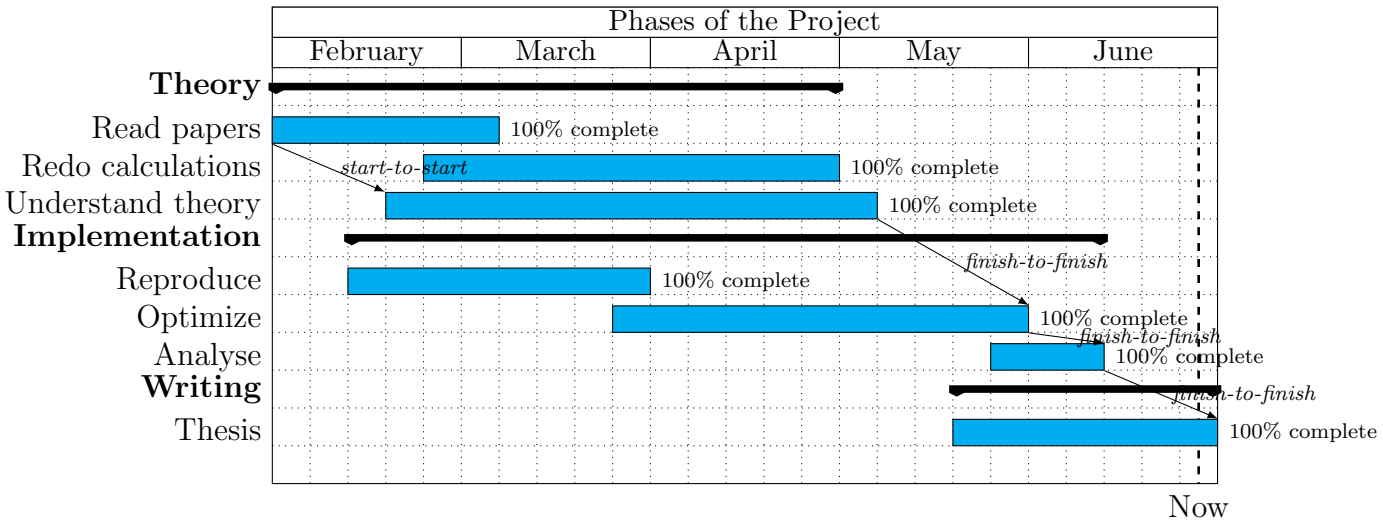

Figure 1: Gantt diagram of the project

2 State of the art

2.1 Anderson localization

In 1958, P. W. Anderson [3] showed that enough structural disorder in a solid-state system, can exhibit localisation of states. Those states present an exponential decaying tail in the probability density function, which leads to the confinement of particles in times much larger than the characteristic time of the system which implies that quantum particles inside such a system can be confined in a region of space in which classical particles are not.

This phenomenon emerges when treating particles as waves, and studying the scattering processes that take place between them. If the disorder is strong enough, the wave function interacts with itself resulting in a constructive interference in a small region of space. Following the Ioffel-Regel criterium found in [4], if the mean free path of a particle is smaller than theh wavelength

$$\lambda \gtrsim l, \tag{2.1.1}$$

the scattering events of the wavefunction will be correlated, and the particle will behave as a wave. In this regime, we can find localization.

This effect has been observed in various systems, such as light in disordered media [5] or water waves in acoustic systems [6]. In fig. 2, we see a setup made in [6] in which they have a shallow water tank set into vibration, with some nails as dispersors. The image represents the shadow casted by the water waves when a light is shone from below. In the first image, the scatterers are placed in a regular pattern, and the system was shaken at 76 Hz. This setup is analogous to the insulating behaviour in a metal. In the second and third images, the scatterers are placed in a random pattern and shaken at two different frequencies: 76 Hz and 105 Hz.

The interesting effect taking place is that when the system is vibrating at 105 Hz, the water waves localize in some regions only in the random pattern, while at 76 Hz, the waves are localized in both patterns. It is also interesting to see that between figures 2 b and 2 c, the localization occurs in different regions of space. A close inspection of the images shows that, for example, the rightmost dispersors in the image 2 c are more sharp, while in 2 b, the dispersors on the left seem to be more defined. This is a visual example of strong localization.

In the case of electrons, Anderson localisation is a fundamental concept in condensed matter physics, as it is expected to be responsible for the insulating behaviour of disordered materials. Understanding this effect is crucial for characterizing electronic transport properties. For example, in the field of semiconductors, InGaN is a material that has been used to create blue LEDs. GaN is a crystalline semiconductor, then the In atoms are randomly distributed in the GaN lattice. The presence of these In atoms creates a random potential in the system, which can lead to electron localization. This is a current research topic in the field of semiconductors.

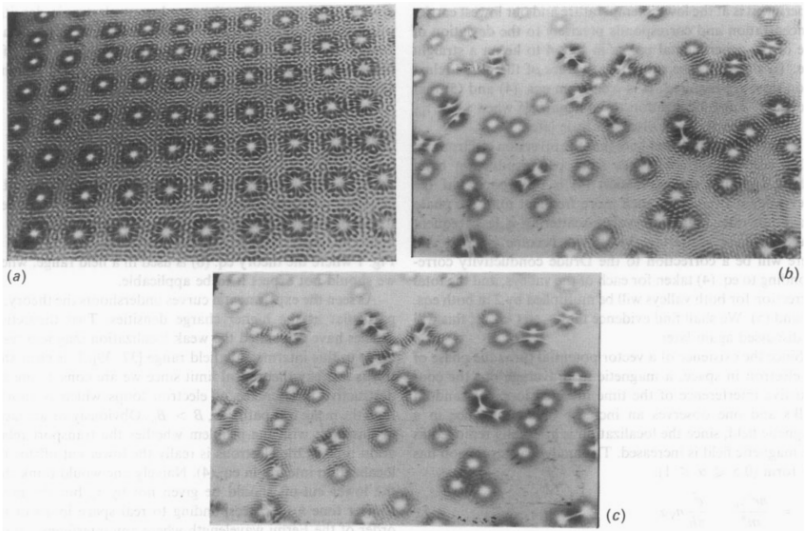

Figure 2: *a)* Periodic lattice of dispersors shaken at 76 Hz. *b)* and *c)* Random lattice of dispersors shaken at 105 and 76 Hz. Figure 5 of [6]

2.2 Ultracold atoms for quantum simulation

Ultracold atoms have been demostrated to be a versatile platform for the study of quantum many-body systems. The ability to control the interactions between atoms, with Feshbach resonances, the external potential, with laser physics, and the temperature of the system, with techniques such as evaporative cooling, allows for the study of a wide range of phenomena and interactions, like superfluidity, bose-einstein condensation, dipolar systems, and many others.

In 2015, Gavish and Castin [7] proposed this platform as a way to study Anderson localisation for a matter wave. The proposal was to build an optical lattice with a low filling factor of an atom B, the scatterers, such that the effect of the lattice would not be noticeable. Then, a second species of atoms A, would be released into this disordered media with a low energy, such that the interaction between A and B would be an s-wave ($l = 0$ in the angular momentum). The scatterers are prepared in the vibrational ground state of the optical lattice, and the atoms A interact with B atoms with a lower energy than the recoil energy of the lattice, such that the interaction is elastic (B atoms don't move). The first approximation to model this kind of s-wave interaction is a delta potential, which is isotropic, meaning that the particles B are modeled as infinitesimally thin scatterers. A representation of the setup in 1D can be seen in fig. 3.

2.3 The pseudopotential approximation. Conditions in the wave function

As stated before, in the setup considered in this work, the interaction between the scatterers and the matter wave is modelled as the typical Yuan and Hang 2D regularized delta-like pseudopotential.

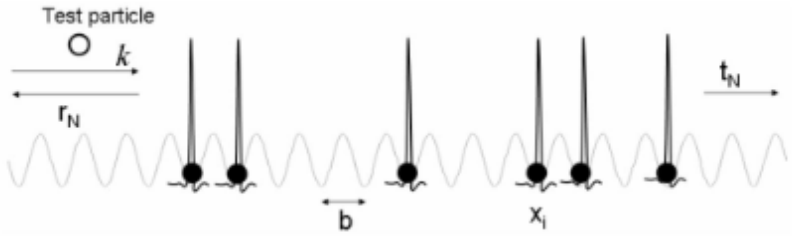

Figure 3: Ultracold atoms in a disordered media. The test particle represents the A atom. This system has a filling factor of 1/3, and the A atoms only see the sharp black potential created by the B atoms. Figure 1 of [7]

The pseudopotential technique consists in approximating a potential with some other easier potential, given some conditions. It is usually used in approximating the Coulomb potential to study it at large distances, as the Coulomb potential has the problem of diverging when $r \to 0$. In fig. 4 one can see an of the application of this technique in a Coulomb pseudopotential. The important idea to take from this is the fact that the behaviour of the wavefunction at large distances from the problem is well reproduced.

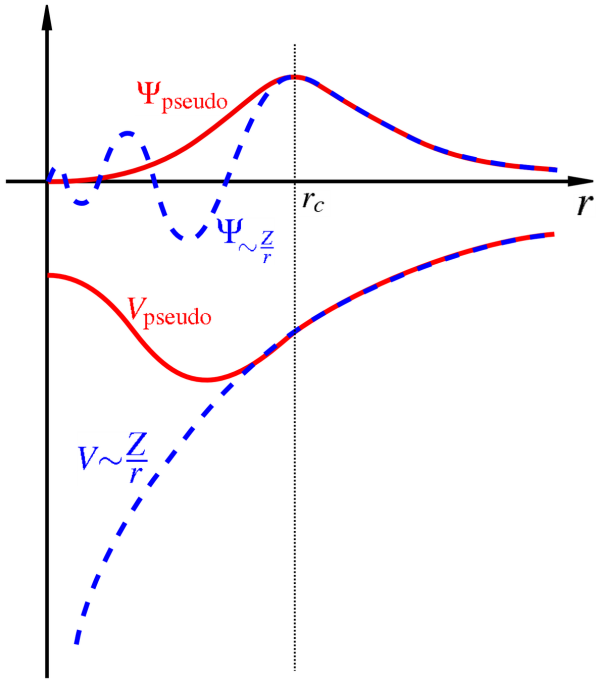

Figure 4: Sketch of the Coulomb potential (blue) and the approximated pseudopotential (red) with their respective wavefunctions. Taken from Wikipedia's pseudopotential page.

In our case, we consider that the B particles are far away from each other, so that the overlap of the wavefunction between B atoms is negligible. For the low filling factor considered, this should be a good approximation. The regularized delta pseudopotential is given by [8]:

$$V(\mathbf{r}) = \frac{\pi\hbar^2}{m}\delta(\mathbf{r})\left(1 - r\ln\left(\frac{r}{2ae^{1-\gamma}}\right)\partial_r\right). \tag{2.3.2}$$

This potential is a first approximation to the problem. We should take into account that this picture is not the full picture of the problem, for example, as this potential is infinitesimally thin, we can't study percolation processes in this system, which could lead to localization of states due to an actual barrier, while with gaussians, if the filling factor is high enough, and the B atoms' wavefunction overlaps, this effect could have a big impact.

The description of the system with this potential, can also be understood in terms of the free Schrödinger equation, with boundary conditions at the position of the scatterers. The Wigner-Bethe-Peierls condition is an equivalent treatment of the problem with this pseudopotential [9] but it has a nicer interpretation. The condition in 2D by a set of scatterers, whose positions are the set $\{\mathbf{r}_i\}$, is described as follows:

$$\psi(\mathbf{r}) = \frac{m}{\pi\hbar^2}D_i\ln\left(\frac{|\mathbf{r}-\mathbf{r}_i|}{a_{eff}}\right) + O(|\mathbf{r}-\mathbf{r}_i|), \tag{2.3.3}$$

which means that we will describe the problem as free particles with these boundary conditions.

2.4 The Fermi gas: Non-interacting fermions

The final objective of this thesis is to study a non-interacting Fermi sea in the presence of disordered scatterers in a finite volume. The Fermi sea is a quantum state of a system of fermions, in which, due to Pauli exclusioin principle, the fermions occupy the lowest energy states available up to a threshold E_F: the Fermi energy E_F, which is defined as the energy of the particle at the Fermi level, that is, the energy of the highest occupied state, and it is strongly related with the number of particles $\mathcal{N}$ in the system.

This means that a Fermi sea can be described as $\mathcal{N}$ free (therefore independent) particles, with the energies allowed by the Pauli exclusion principle. In 2D, the spacing in momentum space is $\delta k = (\frac{2\pi}{L})^2$, where L is the size of the system. Then, the number of states N with momentum less than k is:

$$N = \frac{\pi k_F^2}{\delta k} = \frac{\pi k_F^2}{(\frac{2\pi}{L})^2} = \frac{L^2k_F^2}{4\pi} \tag{2.4.4}$$

where k_F is the Fermi wavevector, defined from the Fermi energy as:

$$E_F = \frac{\hbar^2k_F^2}{2m}. \tag{2.4.5}$$

The Fermi sea can be a good model to study the transport properties of a system at low temperatures. If we suppose that a system is correctly described by a Fermi sea,

the system should be conductor, as the eigenstates of the free particle hamiltonian is an extended state. If we wanted to explain the insulating behaviour of a system, we should consider the interaction between the particles, leading to the usual Fermi-Hubbard model.

But in our case, as Anderson localization is a single particle phenomena, we can have a Fermi sea of non-interacting particles, and even so, find that the system is insulating.

3 Methodology

3.1 Framework used in this work

This work has followed the mathematical formalism started in [7] and followed by [1] and [2].

The main object is the Green's function (or propagator) of the system. This mathematical construct can be suitable for studying the transport properties of systems, as it can be used to solve the Schrödinger equation for a given potential. The free Green's function is defined as the inverse of the operator $E - H_0$, where H_0 is the Hamiltonian of the system and E is the energy of the system (see appendix B).

To do this, we generate the potential by a set of point-like scatterers, in a circular lattice of radius R and distance between scatterers d. An example of a point-like potential can be found in fig. 5. For the diagonalization of the Hamiltonian (see section 4.4), an example of a set of gaussian scatterers can be found in fig. 6.

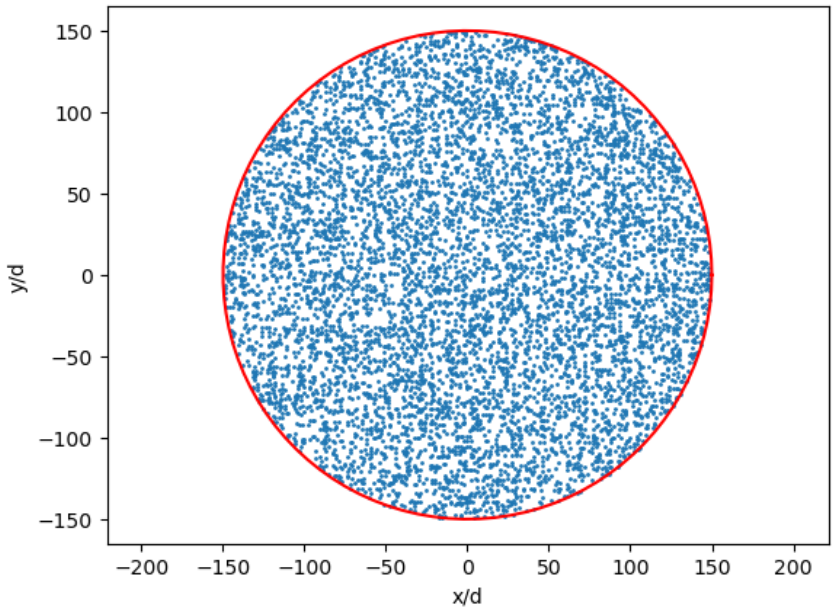

Figure 5: Random point-like potential in a 2D lattice. The scatterers are represented by the blue dots. System with radius $R = 150d$ and filling factor $p_{occ} = 0.1$.

3.2 Criterium for localization

The usual criterium for determining that some state is localized is the exponential decay of the wave function. This can be seen in the Green's function, as if the wavefunction vanishes exponentially, the Green's function will also vanish exponentially.

But, one can see that this criterium could be not enough. Even though it is true that Anderson localization implies an exponential decay of the wave function, there is another situation that leads to this decay: if we inject particles in a spectral gap of the system,

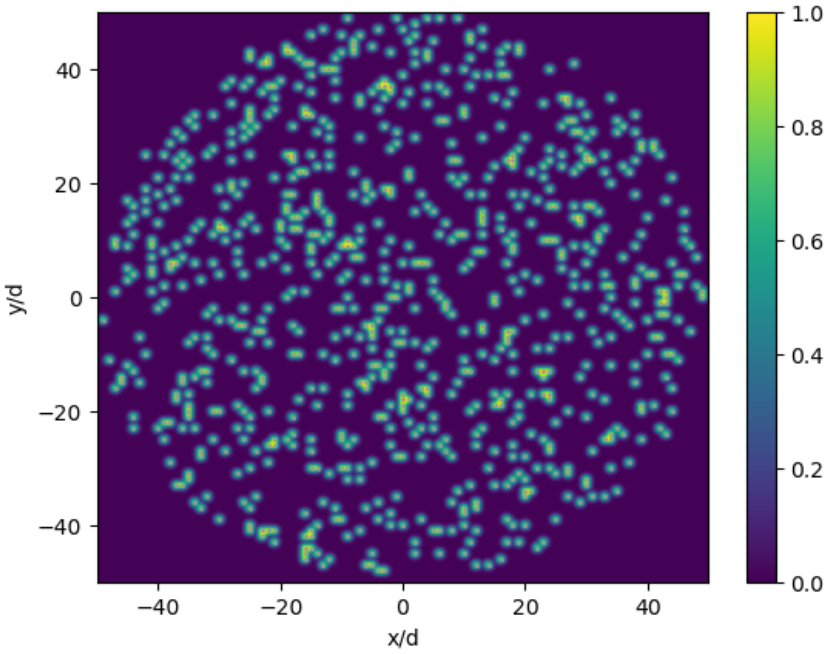

Figure 6: Gaussian potential in a 2D lattice. The color represents the strength of the potential. System with radius $R = 50d$ and filling factor $p_{occ} = 0.1$.

the wave function will decay exponentially. This is not Anderson localization, but a consequence of the spectral gap [10].

3.3 Scaling theory: 2D as a critical dimension

A very elegant argument for understanding localization was put forward by E. Abrahams, P. W. Anderson, D. C. Licciardello, and T. V. Ramakrishnan in [11]. We will discuss this argument following closely the presentation given in [12].

One question that could arise before making the study would be if there even exists such states. Using arguments from the renormalization group technique, we can see that even though 2D is a kind of special dimension, the presence of localized states is expected.

To study the presence of localization in 2D, we can use an argument derived from the renormalization group. The main point is to study the influence of disorder in the electric resistance $V = IR$, where V is the potential applied, R the resistance and I the intensity, and connect the result with the microscopic description of the system $j = \sigma E$, where j is the microscopic current, E the electric field and σ is the conductivity. We define the conductance g as the inverse of the resistance.

$$g = \frac{1}{R} \tag{3.3.6}$$

The conductivity σ could be obtained from first principles and the microscopic description of the system. Following the argument described by the "gang of four" [Gang of four

paper], we will use the argument that the conductance of a block of size $2L$, $g(2L)$, only depends on the conductance of the block of size L, $g(L)$, meaning:

$$g(2L) = f(g(L)) \tag{3.3.7}$$

Supposing this statement is true, we can derive some consequences. We can express the former relation in such a way that no length scale appears:

$$\frac{L}{g}\frac{dg(L)}{dL} = \frac{\mathrm{d}\log(g)}{\mathrm{d}\log(L)} = \beta(g) \tag{3.3.8}$$

Then, for a good concuctor, $g \ll 1$ and we know that ohm's law $R = \rho\frac{L}{A}$ holds. This relation, in fact, fulfills the scaling relation:

$$R = \rho\frac{L}{L^{d-1}} \to g = \sigma_0 L^{d-2} \tag{3.3.9}$$

Where d is the dimension of the system. With this result, in the limit $g \to \infty$ we obtain:

$$\frac{\mathrm{d}\log(g)}{\mathrm{d}\log(L)} = d-2 \to \lim_{g\to\infty}\beta(g) = d-2 \tag{3.3.10}$$

And, following Mott idea, at strong disorder, all wavefunctions are localized, meaning the conductance is expected to behave as:

$$g(L) \propto \exp\{(-L/\xi)\} \Rightarrow \frac{\mathrm{d}\log(g)}{\mathrm{d}\log(L)} = -\frac{L}{\xi} = \log(g) \Rightarrow \lim_{g\to 0}\beta(g) = \log(g) \tag{3.3.11}$$

This argument suggests that below the critical dimension $d = 2$, all states are localized, while above this dimension, there is a critical energy E_c that separates the localized states from the extended states. In fig. 7 we can see the scaling function $\beta(g)$ for dimensions $d = 1, 2, 3$.

3.4 Formulation of the problem

Using the Wigner-Bethe-Peierls condition (or the Huang-Yang delta potential), and the fact that in 2D, $\Delta_{\mathbf{r}}\ln(r) = 2\pi\delta(\mathbf{r})$ the problem is formulated as the usual Green's function for the Schrödinger equation, with secondary point-like sources:

$$\left(z + \frac{\hbar^2}{2m}\Delta_{\mathbf{r}}\right)G(\mathbf{r},\mathbf{r}_0) = \delta(\mathbf{r}-\mathbf{r}_0) + \sum_{i=1}^{N} D_i\delta(\mathbf{r}-\mathbf{r}_i), \tag{3.4.12}$$

where $z \in \mathbb{C}$ is an extension of the energy to the complex plane. The formal solution of this problem is:

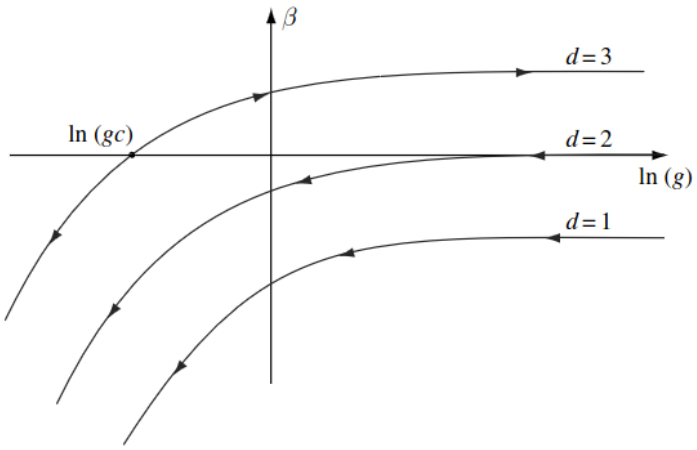

Figure 7: Scaling function of the dimensionless conductance, $\beta(g)$, in dimensions d = 1, 2, and 3. At large values of the conductance, the scaling function approaches the asymptote $\beta(g) \to d-2$ corresponding to ohmic behavior. For very small values of conductance, the scaling function approaches $\beta(g) \to \ln g$, which is characteristic of insulating behavior. According to the weak localization expansion, a localization transition is predicted in dimensions greater than two. Taken from [12]

$$G(\mathbf{r}, \mathbf{r}_0) = g_0(\mathbf{r} - \mathbf{r}_0) + \sum_{i=1}^{N} D_i g_0(\mathbf{r} - \mathbf{r}_i), \tag{3.4.13}$$

where $g_0(\mathbf{r})$ is the 2D free Green's function:

$$g_0(\mathbf{r}) = -\frac{im}{2\hbar^2} H_0^{(1)}(kr). \tag{3.4.14}$$

Then, the secondary source amplitudes D_i are determined by imposing the contact conditions:

$$\sum_{j=1}^{N} M_{ij} D_j = -\frac{\pi\hbar^2}{m} g_0(\mathbf{r}_i - \mathbf{r}_0), \tag{3.4.15}$$

where M_{ij} is the key mathematical object of the problem, defined as:

$$M_{ij} = \begin{cases} \frac{\pi\hbar}{m} g_0(\mathbf{r}_i - \mathbf{r}_j) & i \neq j \\ -\mathrm{i}\frac{\pi}{2} + \ln\left(\frac{k a_{eff} e^{\gamma}}{2}\right) & i = j \end{cases} \tag{3.4.16}$$

where a_{eff} is the effective scattering length of the system, and γ is the Euler-Mascheroni constant. The derivation of this matrix comes from the expansion of the propagator up to second order in the Dyson equation.

Then, the formal solution eq. (3.4.13) can be expressed in terms of this M matrix, which just depends on the configuration of the scatterers, by inverting it:

$$G(\mathbf{r},\mathbf{r}_0) = g_0(\mathbf{r}-\mathbf{r}_0) - \frac{\pi\hbar^2}{m}\sum_{i=1}^{N}\left(\sum_{j=1}^{N} M_{ij}^{-1} g(\mathbf{r}_j-\mathbf{r}_0)\right) g_0(\mathbf{r}-\mathbf{r}_i). \tag{3.4.17}$$

Rearranging terms, it can be expressed as:

$$G(\mathbf{r},\mathbf{r}_0) = g_0(\mathbf{r}-\mathbf{r}_0) - \frac{\pi\hbar^2}{m}\sum_{i,j=1}^{N} g_0(\mathbf{r}-\mathbf{r}_i) M_{ij}^{-1} g(\mathbf{r}_j-\mathbf{r}_0). \tag{3.4.18}$$

And we can write the matrix M in its diagonal basis, such that $M_{ij}^{D} = \delta_{ij} m_i$, where m_i are the eigenvalues of the matrix M. When a matrix is diagonal, the inverse of the matrix is also diagonal, and the diagonal elements are the inverse of the diagonal elements of the original matrix. Then, we can write the i,j-th element of M^{-1} as $M_{ij}^{-1} = \sum_{n=1}^{N} \frac{1}{m_n} D_i^{(n)} D_j^{(n)}$ with $D_i^{(n)}$ being the i-th component of the eigenvector associated to the n-th eigenvalue. Finally, the Green's function can be written as:

$$G(\mathbf{r},\mathbf{r}_0) = g_0(\mathbf{r}-\mathbf{r}_0) - \frac{\pi\hbar^2}{m}\sum_{i,j=1}^{N} g_0(\mathbf{r}-\mathbf{r}_i)\sum_{n=1}^{N}\frac{1}{m_n} D_i^{(n)} D_j^{(n)} g(\mathbf{r}_j-\mathbf{r}_0). \tag{3.4.19}$$

The propagator in quantum mechanics can also be described as the inverse of the operator $E - H_0$, where H_0 is the Hamiltonian of the system and E is the energy of the system (see appendix B). The Green's function expansion in eigenstates of the hamiltonian is:

$$G(\mathbf{r},\mathbf{r}_0) = \sum_n \frac{\psi_n(\mathbf{r})\psi_n^*(\mathbf{r}_0)}{E-E_n}. \tag{3.4.20}$$

If we analytically extend the energy to the complex plane $E \to z \in \mathbb{C}$, we can see that the poles of the Green's function are the eigenvalues of the Hamiltonian. Given a particular complex energy z_{res}, we say a state is a resonance of the system if the Green's function has a pole at that energy. The Green's function can be written as:

$$G(z \to z_{res};\mathbf{r},\mathbf{r}_0) \sim \frac{\psi_{res}(\mathbf{r})\psi_{res}^*(\mathbf{r}_0)}{z-z_{res}}, \tag{3.4.21}$$

which means that a pole in the Green's function is a resonance of the system, which means a state with a very long lifetime. Inspecting eq. (3.4.19), we can see that if a given eigenvalue of the matrix M is zero, the Green's function will have a pole at that energy. This is the criterium used to find the localized states in the system. The problem has been reduced to a problem of finding the eigenvalues of the matrix M.

3.4.1 Wavefunction of a resonance

Given a set of random diffusers, the matrix M can have some eigenvalue which is zero $m_0(z_{res}) = 0$. In this case, we can write the wavefunction in a small region around the complex energy z_{res} comparing the functional form of eq. (3.4.21) and eq. (3.4.19). First of all, we can see that if $m_0(z_{res}) = 0$, $\frac{1}{m_0(z_{res})} \sim \infty$, then $M_{ij}^{-1} = \frac{1}{m_0(z_{res})} D_i^{(0)} D_j^{(0)}$. Taking the Talyor series of $m_0(z)$ around z_{res}, we can see that:

$$m_0(z) = \cancelto{0}{m_0(z_{res})} + m_0'(z_{res})(z - z_{res}) + \dots \tag{3.4.22}$$

Thus, the Green's function can be written as:

$$G(z \to z_{res}; \mathbf{r}, \mathbf{r}_0) \sim -\frac{\pi\hbar^2}{m} \sum_{i,j=1}^{N} g_0(\mathbf{r} - \mathbf{r}_i) \frac{1}{m_0'(z_{res})(z - z_{res})} D_i^{(0)} D_j^{(0)} g(\mathbf{r}_j - \mathbf{r}_0). \tag{3.4.23}$$

And comparing with eq. (3.4.21), we can see that the wavefunction of a localized state is proportional to:

$$\psi_{res}(\mathbf{r}) \propto \sum_{i=1}^{N} g_0(\mathbf{r} - \mathbf{r}_i) D_i^{(0)}. \tag{3.4.24}$$

3.5 Finding resonances

To find the localized states, we could build the matrix M for some (complex) energies, and check its eigenvalues. Even though this could be a method which this work tried, and it is explored in [1], we will use the one step Newton method proposed in [2]. The problem is to find the energy E_{res} such that:

$$m_i(E_{res}) = 0, \tag{3.5.25}$$

where m_i is an eigenvalue of the matrix M. Before trying to find the energy, we have to notice that M depends also on the scattering length a_{eff}, but, using the properties of logarithms, we can split the matrix M in two parts, one that depends on the energy and another that depends on the scattering length:

$$M(E, a_{eff}) = \ln \frac{a_{eff}}{d} \mathbb{I} + M^{\infty}, \tag{3.5.26}$$

which is the same procedure as in [1], but in 2D. Notice then that, because any basis is an eigenbasis of the identity matrix, the eigenvalues of the matrix M are the eigenvalues of the matrix M^{∞} plus $\ln(a_{eff}/d)$:

$$m_i(E, a_{eff}) = m_i^{\infty}(E) + \ln \frac{a_{eff}}{d}. \tag{3.5.27}$$

From here, the Newton step is computed as:

1. Choose an initial energy guess $E \in \mathbb{R}$.
2. Compute a_{eff} such that the real part of $m_i(E)$ is zero:

$$\ln \frac{a_{eff}}{d} = -\mathrm{Re}(m_i^{\infty}(E)) \Rightarrow a_{eff}/d = \exp(-\mathrm{Re}(m_i^{\infty}(E))) \tag{3.5.28}$$

3. Then, z_{res} can be computed as:

$$z_{res} = E - \mathrm{i}\frac{\mathrm{Im}(m_i^{\infty}(E))}{\frac{dm_i^{\infty}}{dE}} \tag{3.5.29}$$

To compute the derivative of the eigenvalue, we can use the Hellmann-Feynman theorem, which states that the derivative of the eigenvalue of a matrix with respect to a parameter is the expectation value of the derivative of the potential with respect to the parameter:

$$\frac{dm_i^{\infty}}{dE} = \left\langle D^i \right| \frac{\mathrm{d}M^{\infty}}{\mathrm{d}E} \left| D^i \right\rangle, \tag{3.5.30}$$

where $|D^i\rangle$ is the eigenvector associated to the eigenvalue m_i^{∞}. The derivative of the matrix M^{∞} with respect to the energy is:

$$\frac{\mathrm{d}M^{\infty}}{\mathrm{d}E} = \frac{\mathrm{d}M^{\infty}}{\mathrm{d}k}\frac{\mathrm{d}k}{\mathrm{d}E} = \frac{\mathrm{d}M^{\infty}}{\mathrm{d}k}\frac{1}{k}, \tag{3.5.31}$$

where k is the wavevector of the system. The derivative of the matrix M^{∞} with respect to the wavevector is:

$$\frac{\mathrm{d}M^{\infty}}{\mathrm{d}k} = \begin{cases} \frac{\mathrm{i}\pi}{2} H_1^{(1)}(kr_{ij}) r_{ij} & i \neq j \\ \frac{1}{k} & i = j \end{cases}. \tag{3.5.32}$$

The result of the algorithm can be compared with eq. (4.2.34), where we can see that the imaginary part of the energy corresponds to the time width of the resonance. Following [2], we see that if the imaginary part of this operation is small enough, the method converges in just a single step. For the real part, we checked that when doing the histogram (see fig. 8), the shift in the value after the step, and the initial guess was smaller than the bin size used, and could be neglected.

4 Results

4.1 Optimization of the code

The first bottleneck found in the process of computing the histogram was the construction of the matrix M itself. In the first iterations of the code we weren't considering the possibility of parallelizing, or even vectorizing the operations. When speaking of *vectorizing* we refer to the use of numpy arrays and operations, which are optimized for numerical operations.

The initial implementation of the M matrix calculation consisted on computing the matrix elements in a serial way, applying the hankel function to each element of the matrix. The approximate time of computing the whole matrix of dimension $N \times N \approx 700 \times 700$ was around 20 seconds. Then, exploiting the fact that the matrix is symmetric, the time was reduced to around 10 seconds.

After this, an arcaic parallelisation scheme was proposed: the matrix was divided in four triangular blocks, and each block was computed in a different process. This computation was done initializing 4 different jobs with the multiprocessing library, and then joining the results. With this we achieved a time of 2.5 seconds for the whole matrix. Even though, the time was reduced by a factor of 8, it was still the bottleneck of the computation.

Finally, thanks to some training done externally, and by rethinking the way in which the matrix is constructed, the construction stopped being the bottleneck. With the help of the fact that numpy and scipy functions are optimized to work with array-like data, the construction was thought as follows:

1. From the list of scatterers (array of dimension $(N, 2)$ consisting on 2D vectors representing the coordinates of each scatterer) an upper diagonal matrix (without diagonal) is constructed, consisting on the value of the distance of dispersor i with dispersor j. That is:
$$\mathcal{D}_{ij} = \begin{cases} |r_i - r_j| & i < j \\ 0 & else \end{cases} \tag{4.1.33}$$
This matrix is computed using numba's njit decorator [13].
2. This matrix is then multiplied by the momentum of the free particle. This basically is an upper triangular matrix that contains the argument of the hankel function.
3. Then, the hankel function is applied once to the whole matrix, reducing the for loops needed.
4. The transposed matrix is added to the upper triangular matrix.
5. Finally, the diagonal is added.

4.2 Density of localized states

The sign of a localized state is the exponential decay of the wavefunction $\psi \propto e^{-\frac{r}{\xi}}$ far from the source. When working with the Green's function, we don't work with exactly

the wavefunction, but with the correlation function. In this case, a localized state has an exponential decay of the correlator, but the exponential decay of the correlator does not imply localization. This is because the state can lie in a spectral gap of the system, where the correlator decays exponentially, and, in fact, this is shown in the appendix A of [1].

In the scope of this study, we will study the density of localized states, that is, we will study the presence of localized states as a function of the energy E of the matter wave. This study lets us discard the spectral gap, as the spectral gap is an energy range in which no state is allowed.

Following [2], a localized state is expected to correspond to a very narrow resonance inside the scattering medium. That is, a localized state corresponds to a pole of the analytically continued Green's function in the lower plane $\Gamma > 0$:

$$z_{res} = E_{res} - i\hbar\frac{\Gamma}{2} \tag{4.2.34}$$

Using a disordered circular lattice of scatterers of radius $R = 150d$ and occupation probability $p = 0.1$, for a mean number of scatterers $\langle N \rangle \approx 7 \cdot 10^3$, we can compute for some energies the mean width of the resonances found. The results are shown in fig. 8. By construction of the matrix M, we can see that the number of eigenvalues of the matrix is equal to the number of dispersors, meaning in this case that we will have for each energy E around $7 \cdot 10^3$ potential resonances. Applying the Newton's method mentioned before, we can identify a scattering length a_{eff} for each eigenvalue of the matrix, which is shown in fig. 9. It is interesting to note that for a small value of the energy, the number of states found for $a_{eff} < d$ (or $\ln(a_{eff}/d) < 0$) is zero, meaning that there are no states available there. For this reason, we will particularize on the states with $a_{eff} = d$.

We can define the surface participation ratio as:

$$S_p = \frac{1}{\rho \sum_{i=1}^{N} |D_i|^4} \tag{4.2.35}$$

Where $\rho \equiv \frac{p_{occ}}{d^2}$ is the average density of scatterers, and D_i is the i-th component of the eigenvector corresponding to the state. Looking at the wavefunction eq. (3.4.24), we can see that this quantity is inversely proportional to the Inverse Participation Ratio, which in general is defined as:

$$IPR = \sum_{i=1}^{N} |\psi_i|^4 \tag{4.2.36}$$

And it is a usual metric to determine how much a state is spread through the system. In lattice systems, an IPR of 1 means that the state is localized in a single site, while an IPR of N^{-1} means that the state is spreaded through all the system.

Then, if we search for states with $S_p^{\frac{1}{2}} < \alpha d^2$, with $\alpha > 0$, we will throw away states which are spreaded through the system.

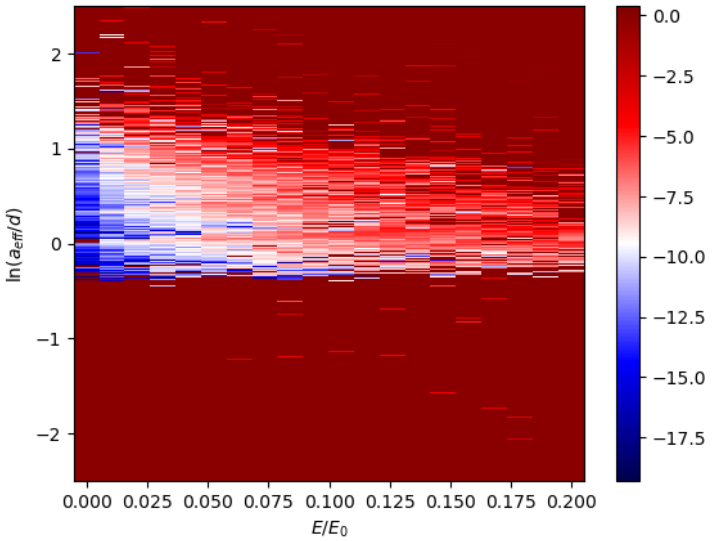

Figure 8: Width Γ of the resonances as a function of the energy E of the matter wave. The color of each bin is computed as the base 10 logarithm off the arithmetic mean of the width of the resonances in that bin, that is, for each bin i we compute $\log_{10}\left(\frac{1}{N_i}\sum_{j\in i}\Gamma_j\right)$, where N_i is the number of resonances in the bin. The width of the bins is $\delta E = 0.01E_0$ and $\delta \ln a_{eff} = 0.007d$. The system used is a disordered circular lattice of scatterers of radius $R = 150d$ and occupation probability $p = 0.1$. The result has been filtered such that the participation surface of the state is $S_p^{\frac{1}{2}} < 9.5d$.

4.3 The wavefunction

With eq. (3.4.24), we can explore the different kinds of wavefunction that we can find in the system. In fig. 12a we can see the wavefunction of a localized state with energy $E = 0.005E_0$ and scattering length $a_{eff} = d$. As it can be seen in the picture the wavefunction only spans a few units of d around its maximum, and decays exponentially far from the source.

Also, we can see that the inverse of the lifetime, or the Γ is really small. Remembering that the lifetime of a state is $\tau = \frac{1}{\Gamma}$, we can see that the lifetime of the state is really long. This is a typical behaviour of a localized state, as the state is confined in a region of space in which the classical particles are not. We will say that a state is localized if the lifetime of the state is longer than 10^6 times the characteristic time of the system, that is, if $\Gamma < 10^{-6}E_0/\hbar$.

The following found state, fig. 12b, is a state with energy $E = 0.005E_0$ and scattering length $a_{eff} = d$. This state is not localized, but for another reason: because the state is in the border of the system, its lifetime (or the mean time to escape the system) is shorter than the threshold. This is intuitive to think, as if the state is in the border of the system, it will have a higher probability of escaping the system.

A complete delocalization of the state is shown in fig. 12c. This state has energy $E =$

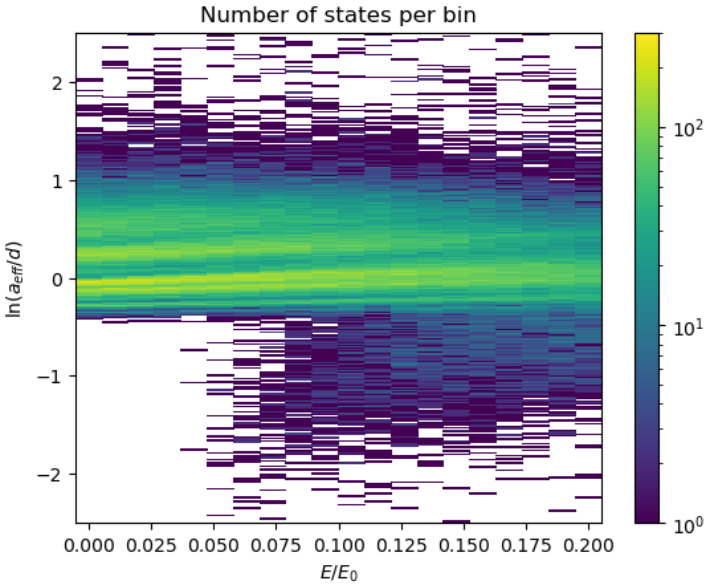

Figure 9: Number of states N_i found for each bin i. The color scale is in logarithm scale, a white value means that no state was found in that bin. The parameters used are the same as in fig. 8.

$0.005E_0$ and scattering length $a_{eff} = d$. The state is spreaded through the whole system, and it is not localized.

As we see in the histogram fig. 8, and can be observed also in [2], as we increase the energy, the number of localized states decreases. An example of a delocalized state is shown in fig. 10, with energy $E = 0.5E_0$ and scattering length $a_{eff} = d$. The state is spreaded through the whole system.

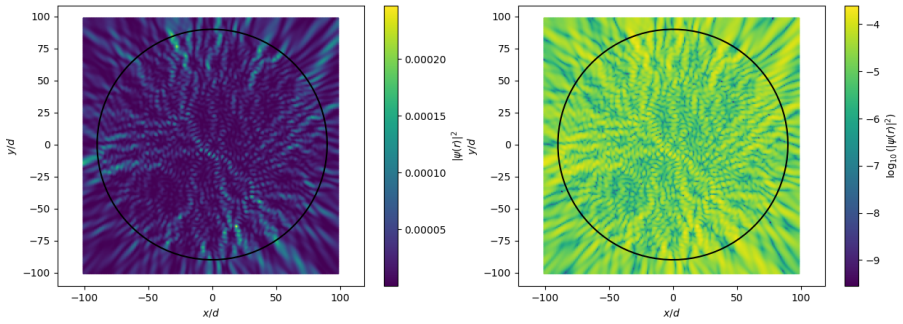

Figure 10: *Left*: Wavefunction of a delocalized state with energy $E = 0.5E_0$ and scattering length $a_{eff} = d$ in a lattice of radius $R = 80d$. *Right* Logarithm of the wavefunction.

Finally, we have to remember that we were computing this inverse of the lifetime with a one step Newton method. This method is only effective for finding resonances with a small width. If at the energy selected, the initial eigenvalue is not small enough, the method

will not converge fast enough.

4.4 Non-interacting fermions

Finally, we can study non-interacting particles inside this system.

To extract the spectrum of the fermi sea in presence of the scatterers, we model the scatterers as very sharp gaussians (see fig. 6), with a width $\sigma = d/4$. The random potential is given by:

$$V(\mathbf{r}) = \sum_i V_i(\mathbf{r}) = \sum_i V_0 \exp\left\{\left(-\frac{|x - r_i^x|^2 + |y - r_i^y|^2}{2\sigma^2}\right)\right\}, \tag{4.4.37}$$

where V_0 is chosen such that:

$$\int g\delta(\mathbf{r}) d^2\mathbf{r} = \int V(\mathbf{r}) d^2\mathbf{r}, \tag{4.4.38}$$

which yields $V_0 = \frac{g}{2\pi\sigma^2}$. Then, we can diagonalize the hamiltonian.

What we will see is if there is a minimum energy E_{min} in which there are no states below. To find it, we can diagonalize the hamiltonian and study the spectrum. In fig. 11 we can see the spectrum of the non-interacting fermions in the system. The minimum energy found is $E_{min} \approx 0.0002E_0$. This energy lies inside the first bin of fig. 8, meaning that there exists states in the first bin.

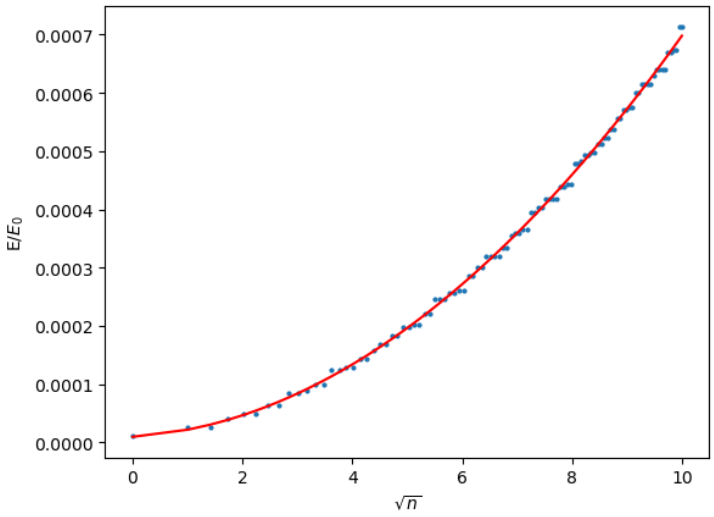

Figure 11: Spectrum of the non-interacting fermions in the system, versus the square root of the index of the eigenvalue. The system used is a disordered circular lattice of scatterers of radius $R = 50d$ and occupation probability $p = 0.1$. The system has been discretized with a grid of $N = 1000 \times 1000$ points.

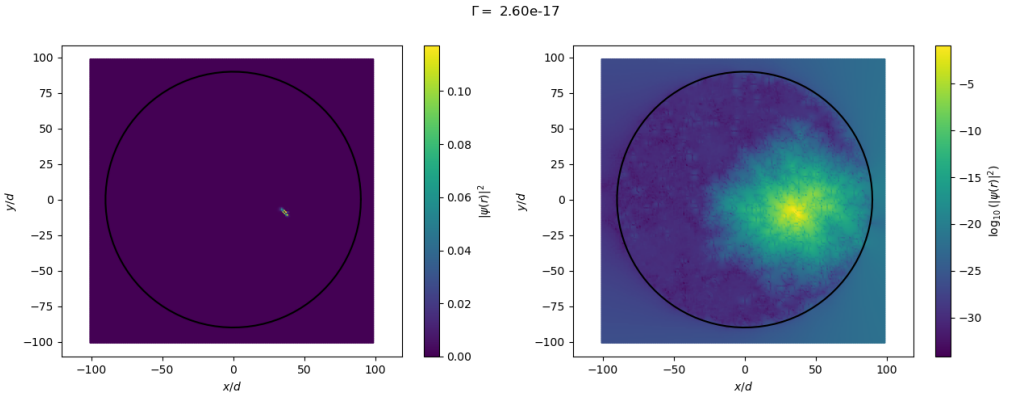

(a) Localized state

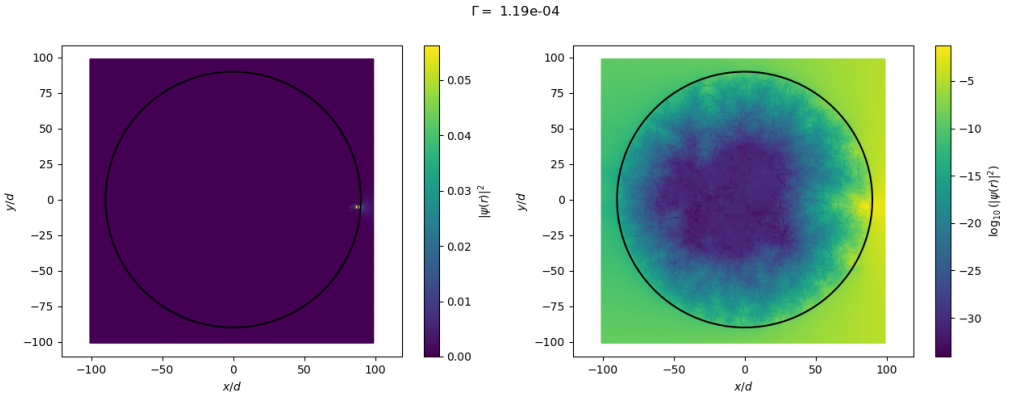

(b) Border state

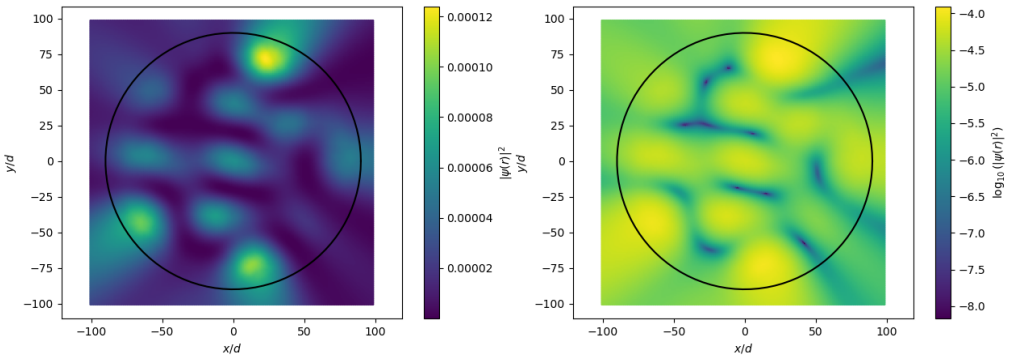

(c) Delocalized state

Figure 12: *Left*: Wavefunction of a state with energy $E = 0.005E_0$ and scattering length $a_{eff} = d$ in a lattice of radius $R = 80d$. *Right* Logarithm of the wavefunction.

5 Budget

The project has been developed in the UPC, using the resources computational resources of the Department of Physics and the personal laptop. The project has not required any additional resources.

6 Environment Impact

As commented before, this thesis has used only computational resources either from a UPC computer or from the personal laptop of the author. The project has not required any additional resources.

It has estimated to have used around 1 week of computational power. Taking an average of 500W of power consumption, the project has used around 84 kWh of energy.

7 Conclusions and future development

This work has explored the Anderson localization phenomenon in a 2D disordered lattice of dispersors in the approximation of a contact interaction between the scatterers and the particles. As the phenomenon is a single particle interference effect, the study has been focused on the study of a single particle, (with a brief excursion to a non-interacting Fermi gas) in the presence of the disorder.

The results obtained have shown that the system can be insulating in some cases, specially at low energies and scattering lengths around $a_{eff} = d$. The system has been studied in a 2D square lattice, but the disorder can be extended to a full disorder without a lattice, and the results should be similar. The system in 3D has been more studied in the literature, as the 3D case presents a critical energy E_c, called mobility edge, that separates the localized states from the extended states. The 2D case does not have this critical energy, and the system could be insulating at any energy, if the disorder was infinite.

The results have been obtained using the Green's function method, and the code has been optimized to be fast enough to be useful. The formalism, although a bit unintuitive at first glance, has proved to be useful to study the proposed problem, and the results have been consistent with the literature.

Personally, the most challenging part of the work has been the formalism of scattering theory in 2D, which is not the most common case in the literature. Other challenges have involved the optimization of the code, which has been one of the most time-consuming parts of the project, as the initial knowledge in efficient programming paradigms (such as parallelisation or vectorization) was not enough to understand why the first iterations of the code were not useful.

In general, this work has been a good introduction to the study of Anderson localization, and the formalism of scattering theory.

Of course, further work implies the calculation of the effective mass of the fermions in the system, but also, the study of this systems can be extended in a lot of ways. The first way could be to not consider the scatterers as point-like, but as a gaussian potential, which could lead to more richer physics in the system. If this was done, the formulation would change from top to bottom, as the matrix M would not be present, and the analytical computations of the perturbative terms in the Dyson equation of the Green's function should be computed, but at the limit of dilute and narrow scatterers, those results should be retrieved. If we wanted to stay in the 2D point-like system, we could have studied the dependence of the density of localized states with the occupation probability.

Appendices

A Two dimensional scattering: binary collisions

This part tries to be a direct translation of [14].

In the dilute gas, interactions are well described by a binary collision model, where the interaction Hamiltonian is defined as a sum of two-body terms.

$$\hat{H}_{\text{int}} = \frac{1}{2}\sum_{i\neq j} U(\mathbf{r}_i - \mathbf{r}_j) \tag{A.0.39}$$

Then it is straightforward that we must begin describing the problem with two bodies interacting via the potential $U(r)$. The study is simplified by the following remarks:

- Dominant interactions are spherically symmetric, so that $U(r)$ actually only depends on $r = |\mathbf{r}|$. Angular momenutm is conserved in a collision, allowing the two-body problem to be treated with eigenstates of the operator $\hat{\mathbf{L}}$. This is the principle of development in partial waves, identified by the angular quantum number $l \in \mathbb{N}$. Note also that for polarized bosons, the symmetrization of the two-body wave function results in only the even values of l being allowed.
- Atoms are cold so their thermal wavelength λ_T is large compared to the size of the potential, which we call b. In other words, the wavevectors $\mathbf{k}$ relevant, which are of the order of $\frac{1}{\lambda_T}$, verifies $kb << 1$. Furthermore, the potential decays rapidly at large distances (short range potential). Those two properties, ensure that the essential properties of the collision are described by the *s-waves*, that is to say the state corresponding to a relative angular momentum $l = 0$ between the two collisioned particles.

A.1 Variable separation, diffusion amplitude

Consider two identical atoms with mass m. We can introduce the center of mass variables $\mathbf{R}$ and $\mathbf{P}$:

$$\mathbf{R} = \frac{1}{2}(\mathbf{r}_1 + \mathbf{r}_2) \qquad \mathbf{P} = \mathbf{p}_1 + \mathbf{p}_2 \tag{A.1.40}$$

and the relative variables $\mathbf{r}$ and $\mathbf{p}$:

$$\mathbf{r} = \mathbf{r}_1 - \mathbf{r}_2 \qquad \mathbf{p} = \frac{1}{2}(\mathbf{p}_1 - \mathbf{p}_2) \tag{A.1.41}$$

The Hamiltonian of the system can be separated in two terms:

$$\hat{H} = \hat{H}_{CM} + \hat{H}_{rel}, \qquad \hat{H}_{CM} = \frac{\hat{P}^2}{2M}, \qquad \hat{H}_{rel} = \frac{\hat{p}^2}{2\mu} + U(\mathbf{r}) \tag{A.1.42}$$

Where we introduced the total mass $M = 2m$ and the reduced mass $\mu = \frac{m}{2}$. The binary collision problem therefore reduces to the problem of a body of reduced mass μ in the external potential $U(\mathbf{r})$, described by the Hamiltonian $\hat{H}_{rel}$. This is the problem we will solve in the following.

We will focus on asymptotically free states which describe a diffusion process. the formalism of collision theory tells us that any plane wave $e^{i\mathbf{k}\cdot\mathbf{r}}$ is an eigenstate of the Hamiltonian

$$\hat{H}_{rel,0} = \frac{\hat{p}^2}{2\mu} \tag{A.1.43}$$

With eigenvalue $E_{\mathbf{k}} = \frac{\hbar^2 k^2}{2\mu}$, then we can associate an eigenstate $\psi_{\mathbf{k}}(\mathbf{r})$ of $\hat{H}_{rel}$ with the same energy,

$$\hat{H}_{rel}\psi_{\mathbf{k}}(\mathbf{r}) = E_{\mathbf{k}}\psi_{\mathbf{k}}(\mathbf{r}) \tag{A.1.44}$$

this state is written asymptotically as the sum of the incident plane wave and an outgoing spherical (three-dimensional) or cylindrical (two-dimensional) wave:

$$\begin{cases} \text{3D}, 1 \ll kr: & \psi_{\mathbf{k}}(\mathbf{r}) \sim C_0 \left\{ e^{i\mathbf{k}\cdot\mathbf{r}} + f(k)\frac{e^{ikr}}{r} \right\} \\ \text{2D}, 1 \ll kr: & \psi_{\mathbf{k}}(\mathbf{r}) \sim C_0 \left\{ e^{i\mathbf{k}\cdot\mathbf{r}} + f(k)\frac{e^{ikr}}{\sqrt{kr}} \left[-\sqrt{\frac{\mathrm{i}}{8\pi}} \right] \right\} \end{cases} \tag{A.1.45}$$

Where C_0 is a normalization constant. We have taken into account the fact that diffusion takes place essentially in the channel with zero angular momentum (s wave) and therefore we limit ourselves to the case of an isotropic diffused wave. Furthermore, we note that the definition of the diffusion amplitude $f(k)$ is not exactly the same in three and two dimensioins, with the factor $\sqrt{k}$ which apperas explicitly in the two-dimensional case. The definitions adopted here ensures analytical properties that are simple to $f(k)$ [some reference]. Finally, let us point out that the reason for the factor in square brackets in the 2D definition is due to the form found for $f(k)$ in the case of a quasi-2D geometry (more on that later) which will take the form $f(k) \approx \tilde{g}$, where the constant $\tilde{g}$ is the parameter usually used to characterize the strength of interactions in this type of problem.

The diffusion amplitude $f(k)$ therefore determines the properties of the binary collision. To compute it, we have to take the angular average of the Schrödinger equation, noting that $R_k(r) = \frac{1}{4\pi}\int \psi_{\mathbf{k}}(r,\theta,\phi)\sin\theta d\theta d\phi$ in 3D and $R_k = \frac{1}{2\pi}\int \psi_{\mathbf{k}}(r,\phi)d\phi$ in 2D. Then, one arrives to the radial Schrödinger equation:

$$\text{3D:} \qquad \frac{\mathrm{d}^2 R_k}{\mathrm{d}r^2} + \frac{2}{r}\frac{\mathrm{d}R_k}{\mathrm{d}r} + \left[k^2 - \frac{2\mu}{\hbar^2}U(r) \right] R_k = 0 \tag{A.1.46}$$

And

$$\text{2D:} \qquad \frac{\mathrm{d}^2 R_k}{\mathrm{d}r^2} + \frac{1}{r}\frac{\mathrm{d}R_k}{\mathrm{d}r} + \left[k^2 - \frac{2\mu}{\hbar^2}U(r)\right]R_k = 0 \tag{A.1.47}$$

Even though the difference between the 3D and the 2D equation appears to be very minor, with only a factor of 2 difference for the first derivative term, we will see that this difference strongly changes the behaviour of the radial function $R_k(r)$ and the diffusion amplitude $f(k)$. Note that the asymtotic behaviour of the radial function $R_k(r)$ is obtained by the angular mean of eq. (A.1.45):

$$\begin{cases} \text{3D}, 1 \ll kr: & R_k(r) \sim C_0 \left\{ \frac{\sin(kr)}{kr} + f(k)\frac{e^{ikr}}{r} \right\} \\ \text{2D}, 1 \ll kr: & R_k(r) \sim C_0 \left\{ J_0(kr) + f(k)\frac{e^{ikr}}{\sqrt{kr}} \left[-\sqrt{\frac{\mathrm{i}}{8\pi}} \right] \right\} \end{cases} \tag{A.1.48}$$

To simplify our analysis, we will assume that the potential $U(r)$ vanishes beyond the radius b. We will focus on the low energy regime $kb \ll 1$, so that there exists an intermediate region of space

$$b < r \ll k^{-1} \tag{A.1.49}$$

such that the potential $U(\mathbf{r})$ has no influence and where we can do a developement at small values of kr for diffusion states $\psi_k(r)$. In particular, the incident plane wave $e^{i\mathbf{k}\cdot\mathbf{r}} \approx 1$ in this intermediate region.

A.2 The diffusion amplitude in 3D

In this section, we aim to obtain a solution of the Schrödinger equation with the corresponding asymptotic behaviour. To do this, we will proceed in three steps, which we will then use to compute it in the two-dimensional case:

1. **General solutions in the area** $U = 0$. We will place ourselves in the zone $r > b$, where U is negligible. The two functions $\frac{e^{\pm ikr}}{r}$ are exact solutions of the radial equation (as well for $kr \gg 1$ and for $b < r < k^{-1}$), and the general solution is a linear combination of these two functions. In particular, if one looks at the intermediate region $b < r < k^{-1}$, one finds:

$$\frac{e^{\pm ikr}}{r} \approx \frac{1 \pm ikr}{r} = \frac{1}{r} \pm ik \tag{A.2.50}$$

which, by linear combinations, give a convenient basis of solutions in this region[1]:

$$R^{(I)}(r) = 1 \qquad R^{(II)}(r) = \frac{1}{r}, \tag{A.2.51}$$

[1]That can be infered taking the limit $k \to 0$ $U \to 0$ in the radial function, so that the final equation is $rR'' + 2R' = 0$, which integrates into $R'(r) = \frac{C_2}{r^2}$ where C_2 is a constant, and therefore $R(r) = C_1 - \frac{C_2}{r}$, where C_1 is another constant

or

$$R(r) = C_1 - C_2\frac{1}{r}, \tag{A.2.52}$$

Where C_1 and C_2 are constants. The asymptotic shape written in terms of the two functions $\frac{e^{\pm ikr}}{r}$ can be transposed to this intermediate region, since these functions are exact solutions as long as the potential U is negligible and we end up with the form of the radial function:

$$R_k(r) = C_1\left[1 + \frac{f(k)}{r}\right] \tag{A.2.53}$$

- A bit more detail in the last calculation:

  In this intermediate region, $e^{\pm ikr} \approx 1 \pm ikr$. Taking:

  $$R_k(r) \sim C_0\left[\frac{\sin(kr)}{kr} + f(k)\frac{e^{ikr}}{r}\right]$$

  and using $sin(x) = \frac{e^{ix}-e^{-ix}}{2i}$, we get:

  $$R_k(r) \sim C_0\left[\frac{e^{ikr} - e^{-ikr}}{2ikr} + f(k)\frac{e^{ikr}}{r}\right] = C_0\left[\frac{1 + ikr - (1 - ikr)}{2ikr} + f(k)\frac{1 + ikr}{r}\right]$$

  Then this can be expressed as:

  $$R_k(r) \sim C_0\left[1 + f(k)\left(\frac{1}{r} + ik\right)\right]$$

  And as we are in this region, $k \to 0$, we can neglect the term ik and we get the expression for $R_k(r)$.

2. **Zero energy solution**. Let's take $k = 0$ in the radial Schrödinger equation and consider the region $r < b$ where $U(r)$ can't be neglected. As it is a second order differential equation, the space solution is of dimension 2. However, we generally find that a single linear combination of solutions is accepatable if we want to respect the regularity of $R_0(r)$ at $r = 0$. When we follow this solution to the point $r = b$, where U becomes negligible and then the previous asymptotic form becomes relevant, this linear combination imposes the ratio $\frac{C_2}{C_1}$. Defining the three-dimensional diffusion lenght by this ratio $a = \frac{C_2}{C_1}$, the solution for $E = 0$ has the form:

$$R_0(r) = C_1\left[1 - \frac{a}{r}\right] \tag{A.2.54}$$

The diffusioin length is by construction the point in which this asymptotic form vanishes.

3. **Connect solutions for low energy** Let's consider now a solution $R_k(r)$ of low energy $kb \ll 1$ and let us place ourselves in the intermediate zone $b < r < k^{-1}$. The comparison of the asymptotic form of $R_k(r)$ with the solution at zero energy, implies a direct link between the diffusion amplitude $f(k)$ and the diffusion length a:

$$a = -\lim_{k\to 0} f(k) \tag{A.2.55}$$

The total cross section of diffusion by the potential $U(r)$ is the calculated by the balance of probability currents at the input and output and we find $\sigma = 4\pi a^2$. For bosonic particles, the effects of quantum statistics adds a factor of 2 in the result.

A.3 The diffusion amplitude in 2D

Proceeding as the 3D case:

1. **General solutions in the area** $U = 0$. The 2D case is inherently more complicated than the 3D case, because cylindrical waves $\frac{e^{\pm ikr}}{\sqrt{r}}$ are not exact solutions of the corresponding radial equation for $U = 0$. If they were, the lower energy limit would provide the basis of functions $\frac{1}{\sqrt{r}} \pm ik\sqrt{r}$, or the linear combination of $\frac{1}{\sqrt{r}}$ and $\sqrt{r}$. But in the limit $k \to 0$ and $U \to 0$, the radial equation reads $rR'' + R' = 0$, which integrates into $R'(r) = \frac{C_1}{r}$, where C_1 is a constant, and therefore

$$R(r) = C_1 \ln r + C_2, \tag{A.3.56}$$

where C_2 is another constant. To find this result in a more general framework, we note that the radial equation in 2D for $U = 0$ is, in fact, the definition equation for Bessel functions of order 0. Two independent solutions of this equation are the Bessel function of the first kind, $J_0(kr)$, and the Bessel function of the second kind, $Y_0(kr)$. The behavior of the functions $J_0(kr)$ and $Y_0(kr)$ are known for big and small values of kr:

$$kr \gg 1: \quad J_0(kr) \sim \sqrt{\frac{2}{\pi kr}} \cos\left(kr - \frac{\pi}{4}\right)$$
$$Y_0(kr) \sim \sqrt{\frac{2}{\pi kr}} \sin\left(kr - \frac{\pi}{4}\right)$$

and

$$kr \ll 1: \quad J_0(kr) \sim 1$$
$$Y_0(kr) \sim \frac{2}{\pi} \ln(\eta kr)$$

Where $\eta \equiv \frac{e^\gamma}{2}$, with γ the Euler-Mascheroni constant. In particular, every linear combination of $J_0(kr)$ and $Y_0(kr)$ at $kr \ll 1$ is a solution of the described form.

2. **Zero energy solution**. For $k = 0$, and with the presence of a potential $U(r)$, the space of general solutions $R_0(r)$ is of dimension 2. However, the regularity of $R_0(r)$ at $r = 0$ imposes a restriction on the linear combination of solutions. When we extend it beyond the radius $r = b$ this linear combination is connected to a particular linear combination of the type shown in eq. (A.3.56), which can be written as:

$$r > b: \quad R_0(r) = C_1 \ln\left(\frac{r}{a_2}\right) \tag{A.3.57}$$

Where $a_2 \equiv e^{-\frac{C_2}{C_1}}$ is the diffusion length in two dimensions.

3. **Connect solutions for low energy**. Moving to the case in which k is not zero but remains very small in front of b^{-1}. To form an outgoing cylindrical wave, we see from the behaviours of $J_0(kr)$ and $Y_0(kr)$ that we must take a function proportional to the linear combination $J_0(kr) + \mathrm{i}Y_0(kr) \equiv H_0^{(1)}(kr)$. More precisely, we will choose:

$$\text{2D},\ 1 \ll kr: \quad \frac{1}{4\mathrm{i}}[J_0(kr) + \mathrm{i}Y_0(kr)] \sim \frac{e^{ikr}}{\sqrt{kr}}\left[-\sqrt{\frac{\mathrm{i}}{8\pi}}\right] \tag{A.3.58}$$

- A bit more detail in the last calculation: Using the expressions for $J_0(kr)$ and $Y_0(kr)$, in the limit $kr \gg 1$ we have:

$$\begin{aligned}
\frac{1}{4\mathrm{i}}[J_0(kr) + \mathrm{i}Y_0(kr)] &= \frac{1}{4\mathrm{i}}\left[\sqrt{\frac{2}{\pi kr}}\cos\left(kr - \frac{\pi}{4}\right) + \mathrm{i}\sqrt{\frac{2}{\pi kr}}\sin\left(kr - \frac{\pi}{4}\right)\right] \\
&= \frac{1}{4\mathrm{i}}\sqrt{\frac{2}{\pi kr}}\left[\cos\left(kr - \frac{\pi}{4}\right) + \mathrm{i}\sin\left(kr - \frac{\pi}{4}\right)\right] \\
&= \frac{1}{4\mathrm{i}}\sqrt{\frac{2}{\pi kr}}e^{i(kr-\frac{\pi}{4})} = -\mathrm{i}\sqrt{\frac{2}{16\pi}}\frac{e^{ikr}}{\sqrt{kr}}\underbrace{e^{-i\frac{\pi}{4}}}_{\sqrt{i}} \\
&= -(\mathrm{i})\sqrt{\frac{\mathrm{i}}{8\pi}}\frac{e^{ikr}}{\sqrt{kr}}
\end{aligned}$$

Where we can recognize the factor we introduced with the diffusion amplitude. For $r > b$, the desired radial function is therefore of the type

$$R_k(r) = C_0\left[J_0(kr) + \frac{f(k)}{4\mathrm{i}}H_0^{(1)}(kr)\right] \tag{A.3.59}$$

In the intermediate region $b < r < k^{-1}$, this linear combination becomes:

$$R_k(r) = C_0\left[+\frac{f(k)}{4\mathrm{i}}\left(1 + \mathrm{i}\frac{2}{\pi}\ln(\eta kr)\right)\right] \tag{A.3.60}$$

Which, in the limit of $k \to 0$, the diffusion amplitude is given by:

$$f(k) = -4\mathrm{i}\frac{1}{1 + \mathrm{i}\frac{2}{\pi}\ln(\eta k a_2)} = \frac{1}{-\frac{1}{2\pi}\ln(\eta k a_2) + \frac{\mathrm{i}}{4}} \tag{A.3.61}$$

So that we recover the form found earlier $C_1 \ln\left(\frac{r}{a_2}\right)$ with, in particular, $R_k(r) = 0$ at $r = a_2$.

Note that the diffusion amplitude $f(k)$ tends towards 0 at small k, unlike the 3D case where it tended towards a finite limit equal to $-a$. Furthermore, the total cross section of diffusion by the potential $U(r)$ is also calculated here by a balance of the probability currents at the input and output. We find $\sigma(k) = \frac{|f(k)|^2}{4k}$, which has the dimension of length and diverges gradually with the decrease of k.

B Green's function

B.1 Definition

This work has been developed using the *Green's function method* for solving non-homogeneous differential equations.

Given a differential equation of the form $\mathcal{L}u(x) = f(x)$, where $\mathcal{L}$ is a *linear differential operator* acting on distributions over a subset Ω of the euclidean space $\mathbb{R}^n$, the Green's function at point $s \in \Omega$ is defined as:

$$\mathcal{L}G(x,s) = \delta(x-s) \tag{B.1.62}$$

These functions are a useful tool in wave mechanics, as they can be used to solve differential equations of the form:

$$\mathcal{L}u(x) = f(x) \tag{B.1.63}$$

Theorem B.1. *Given a Green's function $G(x,s)$ that corresponds to the linear differential operator $\mathcal{L}(x)$, the solution of the problem B.1.63 is given by:*

$$u(x) = \int_\Omega G(x,s)f(s)ds \tag{B.1.64}$$

Proof. Starting from the definition of the Green's function, we can integrate by $\int_\Omega f(s)ds$:

$$\int_\Omega \mathcal{L}(x)G(x,s)f(s)ds = \int_\Omega \delta(x-s)f(s)ds \tag{B.1.65}$$

Given that $\mathcal{L}$ is linear in x, and using the properties of the δ distribution, we have:

$$\mathcal{L}\int_\Omega G(x,s)f(s)ds = f(x) \tag{B.1.66}$$

And one can identify that:

$$u(x) = \int_\Omega G(x,s)f(s)ds \tag{B.1.67}$$

Where the Green's function $G(x,s)$ satisfies the same boundary conditions as $u(x)$. □

An important fact to notice is that if the differential operator's coefficients are constant with respect of the independent variable x, the system is transnational invariant and the Green's function is just a function of a single variable:

$$G(x,s) = G(x-s) \tag{B.1.68}$$

B.2 Green's function in quantum mechanics: The single particle propagator

Taken from [15].

Knowing the Green's function method, we can apply it to the well known time-independent Schrödinger equation in the position representation. Given a Hamiltonian $H_0(\mathbf{r})$, the eigenstates of which are known, we can write the Schrödinger equation as:

$$(H_0(\mathbf{r}) + V(\mathbf{r}))\Psi_E(\mathbf{r}) = E\Psi_E(\mathbf{r}) \tag{B.2.69}$$

This is a useful representation of the scattering problems, where $H_0(\mathbf{r})$ is the initial Hamiltonian and $V(\mathbf{r})$ would be the potential that scatters the particles. We can rewrite the equation as:

$$(E - H_0(\mathbf{r}))\Psi_E(\mathbf{r}) = V(\mathbf{r})\Psi_E(\mathbf{r}) \tag{B.2.70}$$

Which is a non-homogeneous differential equation of the form of eq. (B.1.63), where the source term is $V(x)\Psi_E(\mathbf{r})$. The Green's function for the time independent Schrödinger equation is defined as:

$$(E - H_0(\mathbf{r}))G_0(\mathbf{r}, \mathbf{s}; E) = \delta(\mathbf{r} - \mathbf{s}) \tag{B.2.71}$$

Where it is natural to define the inverse of $G_0(\mathbf{r}, \mathbf{s})$ as the operator $E - H_0(\mathbf{r})$. To be rigurous, the inverse of the Green's function is defined as:

$$G_0^{-1}(\mathbf{r}, \mathbf{s}; E) = (E - H_0(\mathbf{r}))\delta(\mathbf{r} - \mathbf{s}) \equiv G_0^{-1}(\mathbf{r}) \tag{B.2.72}$$

This representation is just a way of saying that the inverse of the Green's function is diagonal in the position representation. With this definition, we can see that it is in fact the inverse of the Green's function:

$$\begin{aligned}\int_\Omega G_0^{-1}(\mathbf{r}, \mathbf{s}; E)G_0(\mathbf{s}, \mathbf{y}; E)ds &= \int_\Omega (E - H_0(\mathbf{r}))\delta(\mathbf{r} - \mathbf{s})G_0(\mathbf{s}, \mathbf{y}; E)ds \\ &= (E - H_0(\mathbf{r}))G_0(\mathbf{r}, \mathbf{y}; E) = \delta(\mathbf{r} - \mathbf{y})\end{aligned} \tag{B.2.73}$$

Then, the Schrödinger equation can be rewritten as:

$$\left(G_0^{-1}(\mathbf{r}; E) - V(\mathbf{r})\right)\Psi_E(\mathbf{r}) = 0 \tag{B.2.74}$$

With:

$$G_0^{-1}(\mathbf{r}; E)G_0(\mathbf{r}, \mathbf{y}; E) = \delta(\mathbf{r} - \mathbf{y}) \tag{B.2.75}$$

Proposition B.2. The solution of the Schrödinger equation is given by:

$$\Psi_E(\mathbf{r}) = \Psi_E^0(\mathbf{r}) + \int_\Omega G_0(\mathbf{r},\mathbf{s};E)V(\mathbf{s})\Psi_E(\mathbf{s})d\mathbf{s} \tag{B.2.76}$$

Where $\Psi_E^0(\mathbf{r})$ is the solution of the homogeneous equation.

Proof. We can substitute the proposed solution (eq. (B.2.76)) into the Schrödinger equation eq. (B.2.74):

$$\big(G_0^{-1}(\mathbf{r};E) - V(\mathbf{r})\big)\left(\Psi_E^0(\mathbf{r}) + \int_\Omega G_0(\mathbf{r},\mathbf{s};E)V(\mathbf{s})\Psi_E(\mathbf{s})d\mathbf{s}\right) = 0 \tag{B.2.77}$$

Using the definition of $\Psi_E^0(\mathbf{r})$, we can see that:

$$G_0^{-1}(\mathbf{r};E)\Psi_E^0(\mathbf{r}) = 0$$

As this is just the homogeneous Schrödinger equation. Then, the expression simplifies to:

$$\big(G_0^{-1}(\mathbf{r};E) - V(\mathbf{r})\big)\int_\Omega G_0(\mathbf{r},\mathbf{s};E)V(\mathbf{s})\Psi_E(\mathbf{s})d\mathbf{s} = V(\mathbf{r})\Psi_E^0(\mathbf{r}) \tag{B.2.78}$$

Grouping all terms with the potential $V(\mathbf{r})$, we have:

$$G_0^{-1}(\mathbf{r};E)\left(\int_\Omega G_0(\mathbf{r},\mathbf{s};E)V(\mathbf{s})\Psi_E(\mathbf{s})d\mathbf{s}\right) = V(\mathbf{r})\underbrace{\left(\Psi_E^0(\mathbf{r}) + \int_\Omega G_0(\mathbf{r},\mathbf{s};E)V(\mathbf{s})\Psi_E(\mathbf{s})d\mathbf{s}\right)}_{\Psi_E(\mathbf{r})} \tag{B.2.79}$$

And, using eq. (B.2.75), we have:

$$\int_\Omega \underbrace{G_0^{-1}(\mathbf{r};E)G_0(\mathbf{r},\mathbf{s};E)}_{\delta(\mathbf{r}-\mathbf{s})}V(\mathbf{s})\Psi_E(\mathbf{s})d\mathbf{s} = V(\mathbf{r})\Psi_E(\mathbf{r}) \tag{B.2.80}$$

□

For the time-dependent Schrödinger equation, problem is formulated as:

$$(i\partial_t - H_0(\mathbf{r}) - V(\mathbf{r}))\Psi(\mathbf{r},t) = 0 \tag{B.2.81}$$

Now we can define two operators as follows:

$$(i\partial_t - H_0(\mathbf{r}))G_0(\mathbf{r},\mathbf{s};t-t') = \delta(\mathbf{r}-\mathbf{s})\delta(t-t') \tag{B.2.82a}$$
$$(i\partial_t - H_0(\mathbf{r}) - V(\mathbf{r}))G(\mathbf{r},\mathbf{s};t-t') = \delta(\mathbf{r}-\mathbf{s})\delta(t-t') \tag{B.2.82b}$$

And, following the diagonal notation, we can identify the inverse operators as:

$$G_0^{-1}(\mathbf{r},;t) = i\partial_t - H_0(\mathbf{r}) \tag{B.2.83}$$
$$G^{-1}(\mathbf{r};t) = i\partial_t - H_0(\mathbf{r}) - V(\mathbf{r}) \tag{B.2.84}$$

Then, we can express the self-consistent equation as:

$$\Psi(\mathbf{r},t) = \Psi^0(\mathbf{r},t) + \int d\mathbf{r}' \int dt' G_0(\mathbf{r},\mathbf{r}';t-t')V(\mathbf{r}')\Psi(\mathbf{r}',t') \tag{B.2.85}$$
$$\Psi(\mathbf{r},t) = \Psi^0(\mathbf{r},t) + \int d\mathbf{r}' \int dt' G(\mathbf{r},\mathbf{r}';t-t')V(\mathbf{r}')\Psi^0(\mathbf{r}',t') \tag{B.2.86}$$

With these two equations, one can derive the Dyson equation for the Green's function, which is a fundamental equation in quantum mechanics. Dropping the integrals from eq. (B.2.85), we have:

$$\begin{aligned}\Psi &= \Psi^0 + G_0V\Psi^0 + G_0VG_0V\Psi^0 + G_0VG_0VG_0V\Psi^0 + \dots \\ &= \Psi^0 + (G_0 + G_0VG_0 + G_0VG_0VG_0 + \dots)V\Psi^0\end{aligned} \tag{B.2.87}$$

And comparing it with eq. (B.2.86), we can express the operator G as:

$$G = G_0 + G_0VG_0 + G_0VG_0VG_0 + \dots \tag{B.2.88}$$
$$= G_0 + G_0V(G_0 + G_0VG_0 + \dots) \tag{B.2.89}$$

Wich is just the Dyson equation:

$$G = G_0 + G_0VG \tag{B.2.90}$$

This new operator G is often called the **propagator** of the system. This can be seen starting from the time-dependent Schrödinger equation. For this derivation we will use Dirac notation, where the state of the system is represented by a ket $|\alpha, t_0; t\rangle$, where α is the state of the system and t_0 is the initial time. This section is taken from [16]. The time-dependent Schrödinger equation can be written as:

$$i\hbar\partial_t |\alpha, t_0; t\rangle = \hat{H} |\alpha, t_0; t\rangle \tag{B.2.91}$$

Where $\hat{H} = H_0 + V$ is the Hamiltonian operator of the system. The solution of this equation is given by the operator $\hat{U}(t, t_0) = e^{-\frac{i}{\hbar}\hat{H}(t-t_0)}$. Following Dirac notation, the wave function can be written as:

$$\Psi(\mathbf{r},t) = \langle \mathbf{r}| \hat{U}(t,t_0) |\Psi(t_0)\rangle \tag{B.2.92}$$

Using the completeness relation of the base $1 = \int d\mathbf{r} \, |\mathbf{r}\rangle \langle \mathbf{r}|$ we can express eq. (B.2.92) as:

$$\begin{aligned}\Psi(\mathbf{r},t) &= \int d\mathbf{r}' \, \langle \mathbf{r}| \hat{U}(t,t_0) |\mathbf{r}'\rangle \langle \mathbf{r}'|\Psi(t_0)\rangle \\ &= \int d\mathbf{r}' \, \langle \mathbf{r}| \hat{e}^{-\frac{i}{\hbar}\hat{H}(t-t_0)} |\mathbf{r}'\rangle \, \Psi(\mathbf{r}';t_0),\end{aligned} \tag{B.2.93}$$

which is understood as the amplitude of going from $\mathbf{r}'$ to $\mathbf{r}$, integrated over all possible paths. If we take the Fourier transform [2] we obtain the propagator in the space of energies:

$$G(\mathbf{r},\mathbf{r}';E) = \langle \mathbf{r}| \frac{1}{E - \hat{H} + i\eta} |\mathbf{r}'\rangle \tag{B.2.94}$$

And expanding in the eigenbasis of the hamiltonian we have:

$$G(\mathbf{r},\mathbf{r}';E) = \sum_n \langle \mathbf{r}| \frac{|\psi_n\rangle \langle \psi_n|}{E - E_n + i\eta} |\mathbf{r}'\rangle = \sum_n \frac{\psi_n(\mathbf{r})\psi_n^*(\mathbf{r}')}{E - E_n + i\eta}, \tag{B.2.95}$$

where $\hat{H} |\psi_n\rangle = E_n |\psi_n\rangle$. This last equation is the one used to obtain the wavefunction of a resonance.

[2] The derivation is taken from [16] and it will be skipped for simplicity of the problem

References

[1] Pietro Massignan and Yvan Castin. Three-dimensional strong localization of matter waves by scattering from atoms in a lattice with a confinement-induced resonance. *Physical Review A*, 74(1):013616, July 2006.

[2] Mauro Antezza, Yvan Castin, and David A. W. Hutchinson. Quantitative study of two- and three-dimensional strong localization of matter waves by atomic scatterers. *Physical Review A*, 82(4):043602, October 2010.

[3] P. W. Anderson. Absence of Diffusion in Certain Random Lattices. *Physical Review*, 109(5):1492–1505, March 1958.

[4] B. Kramer and A. MacKinnon. Localization: Theory and experiment. *Reports on Progress in Physics*, 56(12):1469, December 1993.

[5] Diederik S. Wiersma, Paolo Bartolini, Ad Lagendijk, and Roberto Righini. Localization of light in a disordered medium. *Nature*, 390(6661):671–673, December 1997.

[6] P. E. Lindelof, J. Nørregaard, and J. Hanberg. New Light on the Scattering Mechanisms in Si Inversion Layers by Weak Localization Experiments. *Physica Scripta*, 1986(T14):17, January 1986.

[7] U. Gavish and Y. Castin. Matterwave localization in disordered cold atom lattices. *Physical Review Letters*, 95(2):020401, July 2005.

[8] Aaron Farrell and Brandon P. van Zyl. S-wave scattering and the zero-range limit of the finite square well in arbitrary dimensions. *Canadian Journal of Physics*, 88(11):817–824, November 2010.

[9] H. Bethe, R. Peierls, and Douglas Rayner Hartree. Quantum theory of the diplon. *Proceedings of the Royal Society of London. Series A - Mathematical and Physical Sciences*, 148(863):146–156, January 1997.

[10] Matthew B. Hastings and Tohru Koma. Spectral Gap and Exponential Decay of Correlations. *Communications in Mathematical Physics*, 265(3):781–804, August 2006.

[11] E. Abrahams, P. W. Anderson, D. C. Licciardello, and T. V. Ramakrishnan. Scaling Theory of Localization: Absence of Quantum Diffusion in Two Dimensions. *Physical Review Letters*, 42(10):673–676, March 1979.

[12] Alexander Altland and Ben D. Simons. *Condensed Matter Field Theory*. Cambridge University Press, Cambridge, 2 edition, 2010.

[13] Numba's documentation.

[14] Jean Dalibard. Low dimension quantum fluids and Kosterlitz-Thouless transition, 2017.

[15] Henrik Bruus, Karsten Flensberg, Henrik Bruus, and Karsten Flensberg. *Many-Body Quantum Theory in Condensed Matter Physics: An Introduction*. Oxford Graduate Texts. Oxford University Press, Oxford, New York, September 2004.

[16] Willem H Dickhoff and Dimitri Van Neck. *Many-Body Theory Exposed!* WORLD SCIENTIFIC, 2nd edition, 2008.